Active rock glaciers of the contiguous United States: GIS inventory and spatial distribution patterns

Gunnar Johnson[1], Heejun Chang[2], and Andrew Fountain[3]

[1]Environmental Science Department, Portland State University, Portland, Oregon, 97201, USA
[2]Geography Department, Portland State University, Portland, Oregon, 97201, USA
[3]Geology Department, Portland State University, Portland, Oregon, 97201, USA

Correspondence to: Gunnar Johnson (alpinebones@gmail.com)

Abstract. In this study we present the Portland State University Active Rock Glacier Inventory (n = 10,332) for the contiguous United States, derived from the manual classification of remote sensing imagery (Johnson, 2020; https://doi.pangaea.de/10.1594/PANGAEA.918585). Individually, these active rock glaciers are found across widely disparate montane environments, but their overall distribution unambiguously favors relatively high, arid mountain ranges with sparse vegetation. While at least one active rock glacier is identified in each of the 11 westernmost states, nearly 88% are found in just five states: Colorado (n = 3889), Montana (n = 1813), Idaho (n = 1689), Wyoming (n = 839), and Utah (n = 834). Mean active rock glacier area is estimated at 0.10 km^2, with cumulative active rock glacier area totaling 1004.05 km^2. Active rock glaciers are assigned to a three-tier classification system based on area thresholds and surface characteristics known to correlate with downslope movement. Class 1 features (n = 7042, average area = 0.12 km^2) appear to be highly active, Class 2 features (n = 2415, average area = 0.05 km^2) appear to be intermediately active and Class 3 features (n = 875, average area = 0.04 km^2) appear to be minimally active. This geospatial inventory will allow past active rock glacier research findings to be spatially extrapolated, help facilitate further active rock glacier research by identifying field study sites, and serve as a valuable training set for the development of automated rock glacier identification and classification methods applicable to other large regional studies.

1 Introduction

The most well-known elements of the alpine cryosphere are massive ice glaciers and perennial snowfields (simply "glaciers" and "snowfields" hereafter). Likely due to their more nuanced definition and relatively difficult identification, rock glaciers are a lesser known component of the alpine cryosphere, and despite recent evidence that they are far more numerous than glaciers, they remain an under-studied and under-appreciated element of the alpine cryosphere (Duguay et al., 2015). The spatial distributions of glaciers and snowfields of the contiguous U.S. are well understood (Fountain et al., 2017; RGI Consortium, 2017). Conversely, the distribution of rock glaciers of the contiguous U.S. is much less certain. Lacking the brilliantly reflective surfaces of glaciers and snowfields, which in late summer afford strong spectral contrast with immediately adjacent land cover, rock glaciers are challenging to identify remotely using automated methods, making spatial

inventories difficult to compile (Millar and Westfall, 2008). The widely accepted continuum concept places rock glaciers somewhere between glaciers, which are composed almost completely of ice and have a low mineral content, and creeping permafrost, which is composed almost completely of mineral fractions and has a low ice content (Haeberli et al., 2006; Berthling, 2011; Anderson et al., 2018). Virtually all rock glaciers form in cryo-conditioned landscapes, resulting from precipitation, meltwater or groundwater percolating into mechanically weathered debris and subsequently freezing (Francou et al., 1999; Berthling, 2011). This interstitial ice is shielded from direct solar insolation and insulated from warm air temperatures during the melt season by the overlying regolith mantle (Jones et al., 2019a). Provided some fraction of the internal ice content remains frozen through the summer, additional ice is incorporated each winter until a rock glacier is formed. Most researchers consider active rock glaciers, the focus of this study, to be flowing bodies of permafrost, composed of generally regular vertical distributions of coarse talus and granular regolith bound by interstitial ice (Clark et al., 1998, Berthling and Etzelmuller, 2011). In this regard we agree with the genetic rock glacier definition, "the visible expression of cumulative deformation by long-term creep of ice/debris mixtures under permafrost conditions", proposed by Berthling (2011).

Rock glaciers that are not actively flowing due to severely reduced fractions, and in many cases a near total absence, of interstitial ice are commonly referred to as inactive, fossil, or relict rock glaciers. While we do not mean to discount the climatological research interest of inactive rock glaciers, confidently identifying them though remote sensing imagery analysis alone is exceptionally difficult, and results from any such attempts should be further investigated by detailed and direct geophysical field examination (Colucci et al., 2019). In many cases inactive rock glaciers ceased flowing hundreds or thousands of years ago, allowing widespread alpine soil and vegetation community development on their surfaces. Indeed, recent research has shown that when attempting to discriminate active rock glaciers from inactive rock glaciers, surficial vegetation cover is the most statistically significant predictor (Kofler et al., 2020). Additionally, these soils and vegetation readily obscure most of the visual evidence of their past activity readily identifiable through remote sensing image analysis, and as such inactive rock glaciers were intentionally excluded from this active rock glacier inventory due to severe limitations in our ability to confidently identify them based on the methods and data sets employed. However, this active rock glacier inventory can readily and directly be compared to major components of other rock glacier inventories, provided those inventories clearly identify which features are active and which features are inactive. Furthermore, previous rock glacier inventories that have attempted to identify both active and inactive rock glaciers have generally found the two feature types are often colocated, meaning the active rock glacier inventory presented here will be a useful starting point for any future efforts to inventory inactive rock glaciers of the contiguous United States.

Debris-covered glaciers are a landform closely related to active rock glaciers that most researchers have generally defined to essentially be talus-covered alpine glaciers, retaining discrete ice cores with relatively low internal concentrations of regolith (Berthling, 2011). The surficial talus mantling of debris-covered glaciers is generally sourced from mass wasting of over-

steepened lateral slopes, often formerly buttressed by the glacier body, but now unsupported and exposed to the elements due to glacial recession. In most cases, fully mantled debris-covered glaciers with thick and continuous surficial debris layers are virtually indistinguishable from the more traditionally defined active rock glaciers through surface analysis alone, either in the field or based on remote sensing imagery. Generally, fully mantled debris covered glaciers with thick and continuous surficial debris layers can only be confidently identified by direct coring or ground penetrating radar, though debris-covered glaciers with expansive surfaces of exposed ice in their accumulation zones and/or thin and discontinuous surficial debris layers are readily discriminated from active rock glaciers through remote sensing imagery analysis. Additionally, in cases where supraglacial lakes and/or streams are present on the surfaces of debris-covered glaciers, these features can be used to discriminate them from active rock glaciers. The nuances of classifying these two cryospheric feature types (e.g., internal ice fraction thresholds, contiguity and extent of ice cores, etc.) is occasionally debated, but is not an issue we seek to resolve with this inventory (Potter, 1972; Clark et al., 1998; Haeberli et al., 2006; Berthling, 2011). While we have made every effort to exclude debris-covered glaciers from this inventory (Fig.1), our methods cannot completely discriminate between fully mantled debris-covered glaciers that lack expansive surfaces of exposed ice in their accumulation zones or obvious supraglacial lakes/streams and traditionally defined active rock-glaciers. Regardless, virtually all examples of both fully mantled debris-covered glaciers that lack expansive surfaces of exposed ice in their accumulation zones or obvious supraglacial lakes/or streams and traditionally defined active rock glaciers have been shaped by a combination of glacial and periglacial forces at some point in their geologically recent history. Indeed, there is considerable evidence that, especially in a rapidly warming world, debris-covered glaciers often transition into active rock glaciers (Anderson et al., 2018; Jones et al., 2019a). As such, we believe any inadvertent inclusion of fully mantled debris-covered glaciers that lack expansive surfaces of exposed ice in their accumulation zones or obvious supraglacial lakes/streams in this active rock glacier inventory should not dramatically impair the utility of the inventory in furthering understanding of the alpine cryosphere.

In this study we develop and present the Portland State University Active Rock Glacier Inventory (PSUARGI) for the contiguous United States (Johnson, 2020). This inventory will help further define the role of active rock glaciers with respect to alpine climatology, ecology, geomorphology, hydrology, and engineering. Rock glacier responses to climate shifts are beginning to be understood with equal specificity to the climatic responses of glaciers, allowing past climatic conditions on short (Bodin et al., 2009; Sorg et al., 2015) and long time scales (Konrad et al., 1999; Stenni et al., 2007; Matthews et al., 2013) to be inferred from their present condition and distribution. The PSUARGI will also help advance growing ecological interest in rock glaciers as climate refugia for cold-adapted flora and fauna (Caccianiga et al., 2011; Sulejman, 2011; Millar et al., 2013b). Previously studied active rock glaciers have shown they can control major fractions of local regolith transport (Kaab and Reichmuth, 2005; Haeberli et al., 2006). Additionally, rock glacier meltwaters exhibit unique hydrographs (Bajewsky and Gardner, 1989; Pauritsch et al., 2015; Jones et al., 2019b) and hydrochemistry signatures (Millar et al., 2013a; Fegel et al., 2016), as well as also volumetric discharge increases in late summer due to climate change (Caine, 2010). From an anthropogenic perspective, active rock glaciers represent unique engineering challenges, particularly with

regard to the possibility of catastrophic collapse and debris flow generation (Iribarren and Bodin, 2010; Lugon and Stoffel , 2010; Bodin et al., 2017), but they also offer engineering opportunities as reservoirs of construction aggregate and water (Burger et al., 1999).

The regional or continental scale impacts of these and other rock glacier influences identified in previous research on individual active rock glaciers cannot be inferred without an accurate active rock glacier inventory at the same spatial scale. Smaller scale rock glacier inventories have been completed before (Table 1), but the active rock glacier distribution across an area the size of the contiguous U.S. has never been quantified in a comprehensive manner. Where prior rock glacier inventories considered study areas most often measured in dozens, hundreds, or, occasionally, thousands of square kilometers, our active rock glacier inventory evaluates a study area of over 3,000,000 km^2. This study addresses a pressing research question: What is the spatial distribution of active rock glaciers of the contiguous U.S.?

2 Data and Methods

2.1 Study Region and Data Sources

We used Google Earth Pro 7.1.7 (Google Earth, 2018) and ESRI ArcMap 10.4 software (ESRI, 2017) to search for active rock glaciers. Google Earth Pro provides imagery acquired at multiple dates from the early 1990s to present, orthorectified to accurate and easily manipulated three-dimensional surfaces. Quick access to multiple images of the same location, captured at different times of day, during different seasons, and across multiple years facilitated active rock glacier identification certainty. We relied on Google Earth Pro and the three-dimensional elevation models it provides for most identifications, supplementing with National Agricultural Imagery Program (NAIP, 2019) plan-view imagery imported into ArcMap 10.4 when Google Earth Pro imagery was unsuitable due to cloud cover, snow cover, or other issues.

We initially began evaluating all montane regions of the contiguous U.S., but failed to find any evidence of active rock glaciers east of the Rocky Mountain States. Therefore, we focused our efforts on the 11 westernmost states (Arizona (AZ), California (CA), Colorado (CO), Idaho (ID), Montana (MT), New Mexico (NM), Nevada (NV), Oregon (OR), Utah (UT), Washington (WA), Wyoming (WY)). Climatologically, this study region is defined by four zones of the NOAA U.S. Climate Region system (Karl and Koss 1984): the Northwest Climate Region (hereafter "NW Region") of ID, OR and WA; the Southwest Climate Region (hereafter "SW Region") of AZ, CO, NM and UT; the West Climate Region (hereafter "W Region") of CA and NV; and the West North Central Climate Region (hereafter "WNC Region") of MT and WY. The major mountain range in each of the four Regions is the Cascades, Southern Rockies, Sierra Nevada and Northern Rockies, respectively.

2.2 Active Rock Glacier Identification

Because glaciers, snowfields, and active rock glaciers are often co-located (Jones et al., 2019a; Knight et al., 2019; Millar and Westfall, 2019), we used two GIS inventories that identify relevant features to inform target areas for our initial search for active rock glaciers; the Randolph Glacier Inventory (RGI) v6.0 (Fountain et al., 2017; RGI Consortium, 2017) and the National Land Cover Database (NLCD) 2011 (Homer et al., 2015). The RGI is focused only on glaciers, whereas the NLCD identifies any perennial snow or ice feature. From this initial effort and our growing expertise in locating active rock glaciers, we expanded our search areas to explore alpine regions far from any inventoried glaciers or perennial snow or ice features, but that could potentially host active rock glaciers.

Active rock glaciers were identified manually by their distinct surface characteristics (Aoyama, 2005; Haeberli et al., 2006). These characteristics include ridge and swale surface banding resulting from differential flow rates and terminal and lateral slopes over-steepened beyond the angle of repose, presumably cemented by interstitial ice. Common mass wasting processes responsible for individual fragments of regolith traveling downslope result in accumulations at or below the angle of repose. Similar approaches to active rock glacier identification, focusing on surface topography characteristics identified from aerial and satellite imagery, have been applied in other previous research (Eztelmuller et al., 2007; Janke, 2007; Degenhardt, 2009; Janke et al., 2015; Millar et al., 2019).

We focused our inventory efforts on identifying active rock glaciers that, surficially, appear to contain appreciable internal ice fractions and are presently or were recently flowing downslope. We follow previous studies that omit features with expansive bare glacial ice in their accumulation zones or obvious supraglacial lakes/streams as those are clearly debris-covered glaciers, but make no further attempt to discriminate active rock glaciers from fully mantled debris-covered glaciers (Bodin et al., 2010; Berthling 2011, Perucca and Angillieri, 2011). After the exponentially larger study area than any previously investigated, a second major distinction between our active rock glacier inventory and classification system and other previous U.S. rock glacier inventory efforts is that we intentionally attempt to exclude inactive rock glaciers. We ignored potential candidate features lacking over-steepened terminal slopes and/or present evidence of advanced surficial soil development, such as expansive vegetation growth, both of which imply the rock glacier has a small internal ice fraction and has not flowed downslope recently.

When identifying a candidate active rock glacier, plan-view images were initially viewed at 1:2000 scale or better. Once suspected ridge and swale flow banding and over-steepened terminal and lateral slopes were identified, image scale was greatly increased. All available clear sky images of the same scene were then evaluated, with plan views being replaced by oblique views from multiple angles and multiple scales and three-dimensional topography exaggerated by 50%. The perimeter of individual active rock glaciers were manually delineated using Google Earth Pro. Usually, sharp changes in

slope were evident, indicating a perimeter boundary between the thickened ice-bound regolith of the active rock glacier and the surrounding unconsolidated talus of the adjacent slope. Additionally, lower active rock glacier margins often abut well-vegetated terrain. The upper margins are often defined by a change in slope, from the steep slopes of exposed bedrock and unconsolidated talus in the rock glacier accumulation zone to the more gentle slope of the main body of the ice-thickened active rock glacier. Generally, active rock glacier boundary confidence is highest along sharp terminal and lateral margins and lowest along accumulation zones where exposed bedrock is not present. When considering multi-lobate active rock glaciers we focused on distinct accumulation zones to ascribe individual lobes to a given active rock glacier.

Understandably, there can be some disagreement between analysts regarding rock glacier classification. To partially address this ambiguity all features identified as active rock glaciers were subsequently assigned to a three-tier classification system based on surface characteristics known to correlate with downslope movement motivated by deformation of the internal ice-rock matrix (Fig. 2), particularly the presence and extent of ridge and swale flow banding (Haeberli et al., 2006; Brenning et al., 2012; Liu et al., 2013). Class 1 rock glaciers appear to be highly active, exhibit unambiguous, complex and extensive ridge and swale flow banding, and have substantially over-steepened terminal and lateral boundaries. Class 2 rock glaciers appear to be intermediately active, exhibit some pronounced ridge and swale flow banding, and have somewhat over-steepened terminal and lateral boundaries. Class 3 rock glaciers appear to be minimally active, exhibit sparse ridge and swale flow banding, and have intermittently over-steepened terminal and lateral boundaries.

To characterize the topographic characteristics of the individual active rock glaciers identified, elevation data were extracted from the USGS National Elevation Dataset (NED) ⅓ arc-second (≈ 10 m) digital elevation model (USGS, 2017). Topographic variables of elevation, slope, aspect, and insolation were determined using Spatial Analyst tools in ArcMap 10.4 (ESRI, 2017). Active rock glacier area was calculated in km^2, while slope and aspect were calculated in degrees. Aspect was decomposed to an eastness and northness component (Nussear et al., 2009), and solar insolation was calculated in watt-hours per m^2. To characterize the climate of the active rock glaciers, climate data, including air temperature and precipitation, were also extracted from PRISM 1981 - 2010 climate normals (PRISM, 2017) using Spatial Analyst tools in ArcMap 10.4. PRISM data were also used to calculate several derivative atmospheric variables, such as fraction of precipitation falling as snow and mean vapor pressure deficit, using the Raster Calculator tool in ArcMap 10.4. These publicly available climate data have a spatial resolution of 800 m, with an average daily accumulated total precipitation bias of less than 2.5% in the western US, 1961 - 2001 (DiLuzio et al., 2008). Active rock glacier classification and area clustering analysis using Moran's I-statistics helped further describe active rock glacier spatial distributions (Cliff and Ord, 1971; Senn 1976; Tiefelsdorf, 2002).

3 Results

3.1 Overall Distribution

We identified 10,332 active rock glaciers (Class 1 = 7042, Class 2 = 2415, Class 3 = 875) across the western U.S. (Fig. 3, Table 2), after removing 146 small (< 0.01 km^2) Class 3 rock glaciers following glaciological convention of area thresholds (Navarro and Magnusson 2017). Average active rock glacier area is 0.10 km^2 and the average distance between each active rock glacier and its nearest neighbor is 0.69 km. Contiguous U.S. active rock glaciers have an average elevation of 3144.3 m, an average slope of 20.51º, an average eastness of -0.007, and an average northness of 0.066 (Fig.4). Climatically, the average annual active rock glacier precipitation is 350.2 mm, the average air temperature is 0.19 °C, the average dew point temperature is -8.37 °C, and the average vapor pressure deficit is 4.52 hPa (Fig. 4). Differences were noted in rock glacier topographic and climatic attribtes between NOAA Climate Regions (Fig. 5). The overall active rock glacier centroid (41.5332,-110.7083) is located in the southwest corner of the WNC Region (Fig. 3). The centroids of each of the three active rock glacier classes (Class 1 = (41.5112, -110.5556), Class 2 = (41.7012, -111.0141), Class 3 = (41.2470, -111.0942)) can be contained by a minimum bounding area circle with a diameter of 57.7 km. Moran's I analysis shows active rock glacier classifications and areas are significantly clustered (Table 3 and Table 4).

3.1.1 Regional Distributions

In the NW Region, we identified 1993 active rock glaciers (Class 1 = 1293, Class 2 = 512, Class 3 = 188)(Fig. 6). Geographically, the average active rock glacier size is 0.07 km^2, and the average distance between each active rock glacier and its nearest neighbor is 0.99 km. Topographically, the average active rock glacier elevation is 2629.6 m, the average slope is 20.7º, the average eastness is 0.000, and the average northness is 0.109 (Fig. 5). Climatically, the average annual active rock glacier precipitation is 365.4 mm, the average air temperature is 1.06 °C, the average dew point temperature is -7.47°C, and the average vapor pressure deficit is 4.85 hPa (Fig. 5). The NW Region active rock glacier centroid (44.8620, -115.2736) is located in the Sawtooth Mountains of Idaho (Fig. 3). The NW Region centroids of each of the three active rock glacier classes (Class 1 = (44.7208, -114.9471), Class 2 = (45.0615, -115.7468), Class 3 = (45.2899, -116.2301)) can be contained by a minimum bounding area circle with a diameter of 106.3 km (Fig. 6).

In the SW Region, we identified 4870 active rock glaciers (Class 1 = 3291, Class 2 = 1133, Class 3 = 446)(Fig. 7). The average SW Region active rock glacier size is 0.09 km^2, and the average distance between each SW Region active rock glacier and its nearest neighbor is 0.59 km. Topographically, the average active rock glacier elevation is 3490.35 m, the average slope is 20.70º, the average eastness is -0.013, and the average northness is 0.046 (Fig. 5). Climatically, the average annual active rock glacier precipitation is 335.12 mm, the average air temperature is -0.09 °C, the average dew point temperature is -8.92 °C, and the average vapor pressure deficit is 4.50 hPa (Fig. 5). The SW Region active rock glacier centroid (38.9385, -107.3569) is located in the Rocky Mountains of Colorado (Fig. 3). The SW Region centroids of each of

the three active rock glacier classes (Class 1 = (38.9066, -107.2755), Class 2 = (39.0867, -107.5456), Class 3 = (38.7968, -107.4786)) can be contained by a minimum bounding area circle with a diameter of 38.2 km (Fig. 7).

In the W Region, we identified 817 active rock glaciers (Class 1 = 552, Class 2 = 181, Class 3 = 84)(Fig. 8). The average W Region active rock glacier size is 0.12 km^2, and the average distance between each W Region active rock glacier and its nearest neighbor is 0.68 km. Topographically, the average active rock glacier elevation is 3412.2 m, the average slope is 20.9º, the average eastness is -0.001, and the average northness is 0.082 (Fig. 5). Climatically, the average annual active rock glacier precipitation is 367.79 mm, the average air temperature is 0.61 °C, the average dew point temperature is -9.52 °C, and the average vapor pressure deficit is 5.07 hPa (Fig. 5). The W Region active rock glacier centroid (37.5421, -118.6340) is located in the Sierra Nevada of California (Fig. 3). The W Region centroids of each of the three active rock glacier classes (Class 1 = (37.5506, -118.6616), Class 2 = (37.4045, -118.6486), Class 3 = (37.7828, -118.4209)) can be contained by a minimum bounding area circle with a diameter of 48.0 km (Fig. 8).

In the WNC Region, we identified 2652 active rock glaciers (Class 1 = 1906, Class 2 = 589, Class 3 = 157)(Fig. 9). The average WNC Region active rock glacier size is 0.11 km^2, and the average distance between each WNC Region active rock glacier and its nearest neighbor is 0.79 km. Topographically, the average active rock glacier elevation is 2813.0 m, the average slope is 19.9º, the average eastness is -0.002, and the average northness is 0.067 (Fig. 5). Climatically, the average annual active rock glacier precipitation is 361.2 mm, the average air temperature is -0.07 °C, the average dew point temperature is -7.7 °C, and the average vapor pressure deficit is 4.13 hPa (Fig. 5). The WNC Region active rock glacier centroid (45.0260,-110.9904) is located in the Rocky Mountains of Montana (Fig. 3). The WNC Region centroids of each of the three active rock glacier classes (Class 1 = (44.9782, -110.8925), Class 2 = (45.1292, -111.2260), Class 3 = (45.2200, -111.2951)) can be contained by a minimum bounding area circle with a diameter of 41.5 km (Fig. 9).

4 Discussion

4.1 Spatial Distribution Patterns

Individually, contiguous U.S. active rock glaciers are found across widely disparate montane environments, but their overall distribution unambiguously favors relatively high, arid mountain ranges with sparse vegetation. Active rock glacier populations in those regions are denser, and the individual active rock glaciers making up those populations are larger and exhibit surficial evidence of higher activity, than those of active rock glaciers found in humid mountain ranges with copious vegetation. Active rock glaciers of the NW Region are largest and most densely concentrated in the Sawtooth Mountains of Idaho. Active rock glaciers of the SW Region are largest and most densely concentrated in the Front Range and San Juan Mountains of Colorado and the Uinta Mountains of Utah. Active rock glaciers of the W Region are largest and most densely

concentrated in the Sierra Nevada of California. Active rock glaciers of the WNC Region are largest and most densely concentrated in the Beartooth Mountains of Montana and the Absaroka Range of Wyoming.

4.2 Inventory Accuracy

The completeness and accuracy of the active rock glacier inventory were qualitatively and quantitatively supported by numerous field observations and remote sensing classification verification by multiple GIS analysts familiar with the alpine cryosphere generally and rock glaciers specifically. The lead author personally visited more than 50 active rock glaciers during field campaigns for related research, and more than 150 individual active rock glaciers with precise coordinates listed in past peer reviewed research were examined remotely when developing our classification criteria. While developing the inventory, dozens of test areas measuring 500 km^2 or greater in all 11 western states were checked by two other well trained GIS analysts familiar with the alpine cryosphere for "missing" active rock glaciers not originally identified by the lead author, and none were found. When considering the three-class active rock glacier activity classification scheme, a test subset of 60 randomly selected active rock glaciers were classified in isolation using the qualitative classification rules previously described by five GIS analysts familiar with the alpine cryosphere generally and rock glaciers specifically. Individual analyst classifications were then compared using Tukey's HSD test ($\alpha = 0.05$), yielding no significant differences between analyst interpretations. Class 1 rock glaciers showed a 92% agreement between analysts, Class 2 rock glaciers an 87% agreement between analysts, and Class 3 rock glaciers a 79% agreement between analysts.

As this active rock glacier inventory is of unprecedented spatial extent, no analogous previous inventories exist for us to make direct and detailed GIS comparisons to over the entire study region. While smaller regional-scale U.S. rock glacier inventories have been compiled in the past, none of these inventories are publicly available as geospatial data sets. Coarse scale comparisons, however, were completed based on reported findings and figures published in previous studies presenting the aforementioned smaller regional U.S. rock glacier inventories. To compare our active rock glacier inventory and previous regional U.S. rock glacier inventories we created polygons using the corner coordinates of low resolution regional study maps from peer-reviewed articles highlighting one Colorado rock glacier inventory (Janke, 2007) and two California rock glacier inventories (Millar and Westfall, 2008; Liu et al., 2013). Polygons representing the extents of maps from the smaller regional inventories were then used to select simple counts of active rock glaciers identified in our inventory and compare them to counts of rock glaciers reported in the aforementioned studies. The 2007 Colorado inventory reported 28 "active" rock glaciers, the category in that study defined most similarly to our Class 1 classification criteria, in and around Rocky Mountain National Park, while we identified 29 Class 1 rock glaciers in the same region. The 2008 California study reported 184 rock glaciers in the central Sierra Nevada, but used a more inclusive "rock-ice feature" definition, that deliberately includes inactive rock glaciers, than our active rock glacier classification criteria, while we identified 116 active rock glaciers of any class in the same region. The 2013 California study (Liu et al., 2013) reported 67 "active" rock glaciers, a subset of features identified in the 2008 study and the category in that study most similar to our Class 1 classification

criteria, while we identified 88 active rock glaciers in largely the same study region. These three comparisons, and the agreement between the aforementioned inventories and our findings, greatly bolster our confidence in the overall accuracy of the PSUARGI.

5 Data Availability

The PSUARGI geospatial data (Johnson, 2020) is available online via the PANGAEA data repository at https://doi.pangaea.de/10.1594/PANGAEA.918585.

6 Conclusions

We present an active rock glacier inventory much larger in both spatial extent and feature count than any previously completed in the U.S., covering a study area of over 3,000,000 km^2 and identifying 10,332 active rock glaciers. Despite beginning our search for active rock glaciers near glaciers and snowfields, we have made clear through this inventory that the majority of active rock glaciers in the contiguous U.S. are found dozens, if not hundreds of kilometers from these more widely appreciated and better understood features. Indeed, some of the densest active rock glacier distributions are found in mountain ranges that host no glaciers and very few snowfields, such as the Sawtooth Mountains of Idaho and the Uinta Mountains of Utah. Active rock glaciers are ubiquitous across wide swaths of the contiguous U.S. not often acknowledged as being part of the alpine cryosphere, and their importance cannot be underestimated. In the majority of regions of the contiguous U.S. where high, arid peaks well above treeline are found, active rock glaciers are found as well. While this inventory is in no way intended to be the final word on active rock glacier distributions of the contiguous U.S., we believe it will be valuable tool in future research aimed at better understanding the influence of climate change on these areas.

Though our deliberate omission of inactive rock glaciers due to limitations in the analysis techniques and data sets available will undoubtedly preclude some desired applications of this active rock glacier inventory, we believe it represents an import step towards a fuller understanding of rock glaciers of the contiguous U.S. regardless. Several potential uses of this active rock glacier inventory are readily apparent, and we hope all will be explored by the research community in due time. Most immediately, this inventory will allow rapid identification of potential field sites for researchers interested in direct study of individual rock glaciers. Many researchers likely do not appreciate just how close their universities or labs already are to active rock glaciers, and this inventory would also offer powerful insights for any researchers eager to inventory inactive rock glaciers. Water resource managers in the arid western U.S. should also take note of active rock glaciers, as the sizes and locations of these features are likely to play an increasingly important role in changing water supplies (Wagner et al., 2020). Finally, we hope this inventory will aid ongoing refinement and future implementation of truly automated rock glacier

detection methods. The ability to quickly, accurately and objectively identify rock glaciers from presently available remote sensing imagery, without relying on skilled visual image analysts or needing to address the inevitable interpretation disagreements between those analysts, would be an invaluable tool for climatologists, ecologists and many others (Brenning, 2009).

7 Author Contributions

Gunnar Johnson designed the research project, created and analyzed the active rock glacier inventory data, and wrote the manuscript. Heejun Chang and Andrew Fountain designed the research project and edited the manuscript

8 Author Contributions

The authors declare that they have no conflict of interest.

9 Acknowledgements

Kristina Dick, Kelly Hughes, Michelle Neeson, Justin Ohlschlager, and Matthias Weislogel all assisted in verifying active rock glacier classifications.

References

Anderson R., Anderson L., Armstrong W., Rossi M., and Crump S. Glaciation of alpine valleys: The glacier – debris-covered glacier – rock glacier continuum, Geomorphology, 311, 127-142, https://doi.org/10.1016/j.geomorph.2018.03.015, 2018.

Angillieri, M. Application of frequency ratio and logistic regression to active rock glacier occurrence in the Andes of San Juan, Argentina, Geomorphology, 114, 396–405, https://doi.org/10.1016/j.geomorph.2009.08.003, 2010.

Aoyama, M. Rock glaciers in the northern Japanese Alps: Paleoenvironmental implications since the Late Glacial, J. Quaternary Sci., 20(5), 471–484, https://doi.org/10.1002/jqs.935, 2005.

Bajewsky, I. and Gardner, J. Discharge and sediment-load characteristics of the Hilda Rock-Glacier stream, Canadian Rocky Mountains, Alberta, Phys. Geogr., 10, 295–306, https://doi.org/10.1080/02723646.1989.10642384, 1989.

Baroni, C., Carton, A., Seppi, R. and Harris, C. Distribution and behaviour of rock glaciers in the Adamello-Presanella Massif (Italian Alps), Permafrost Periglac., 15(3), https://doi.org/10.1002/ppp.497, 243–259, 2004.

Berthling, I. Beyond confusion: Rock glaciers as cryo-conditioned landforms, Geomorphology, 131, 98–106, https://doi.org/10.1016/j.geomorph.2011.05.002, 2011.

Berthling, I. and Etzelmuller, B. The concept of cryo-conditioning in landscape evolution, Quaternary Res., 75, 378–384, https://doi.org/10.1016/j.yqres.2010.12.011, 2011.

Bodin, X., Thibert, E., Fabre, D., Ribolini, A., Schoeneich, P., Francou, B., Reynaud, L., and Fort, M. Two decades of responses (1986–2006) to climate by the Laurichard rock glacier, French Alps, Permafrost Periglac., 20(4), 331–344, https://doi.org/10.1002/ppp.665, 2009.

Bodin, X., Rojas, F., and Brenning, A. Status and evolution of the cryosphere in the Andes of Santiago (Chile, 33.5º S), Geomorphology, 118(3–4), 453–464, https://doi.org/10.1016/j.geomorph.2010.02.016, 2010.

Bodin, X., Krysiecki, J., Schoeneich, P., Le Roux, O., Lorier, L., Echelard, T., Peyron, M., and Walpersdorf, A. The 2006 collapse of the Bérard Rock Glacier (Southern French Alps), Permafrost Periglac., 28, 209–223, https://doi.org/10.1002/ppp.1887, 2017.

Bolch, T. and Gorbunov, A. Characteristics and origin of rock glaciers in Northern Tian Shan (Kazakhstan/Kyrgystan), Permafrost Periglac., 25, 320–332, https://doi.org/10.1002/ppp.1825, 2014.

Brenning, A., Long S., and Fieguth P. Detecting rock glacier flow structures using Gabor filters and IKONOS imagery, Remote Sens. Environ., 125, 227-237, https://doi.org/10.1016/j.rse.2012.07.005, 2012.

Brenning, A. Benchmarking classifiers to optimally integrate terrain analysis and multispectral remote sensing in automatic rock glacier detection, Remote Sens. Environ., 113, 239–247, https://doi.org/10.1016/j.rse.2008.09.005, 2009.

Burger, K., Degenhardt, J., and Giardino, J. Engineering geomorphology of rock glaciers, Geomorphology, 31, 93–132, https://doi.org/10.1016/S0169-555X(99)00074-4, 1999.

Caccianiga, M., Andreis, C., Diolaiuti, G., D'Agata, C., Mihalcea, C., and Smiraglia, C. Alpine debris-covered glaciers as a habitat for plant life, Holocene, 21(6), 1011–1020, https://doi.org/10.1177/0959683611400219, 2011.

Caine, N. Recent hydrologic change in a Colorado alpine basin: An indicator of permafrost thaw?, Ann. Glaciol., https://doi.org/10.3189/172756411795932074, 51(56), 130–134, 2010.

Clark, D., Steig, E., Potter, N., and Gillespie, A. Genetic variability of rock glaciers, Geogr. Ann. A., 80, 175–182, https://doi.org/10.1111/j.0435-3676.1998.00035.x, 1998.

Cliff, A. and Ord, K. Evaluating the percentage points of a spatial autocorrelation coefficient, Geogr. Anal., 3(1), 51–62, https://doi.org/10.1111/j.1538-4632.1971.tb00347.x, 1971.

Colucci, R., Forte, E., Zebre, M., Maset, E., Zanettini, C., and Guglilmin, M. Is that a relict rock glacier?, Geomorphology, 330, 177-189, https://doi.org/10.1016/j.geomorph.2019.02.002, 2019.

Cremonese, E., Gruber, S., Phillips, M., Pogliotti, P., Boeckli, L., Noetzli, J., Suter, C., Bodin, X., Crepaz, A., Kellerer-Pirklbauer, A., Lang, K., Latey, S., Mair, V., Morra di Cella, U., Ravanel, L., Scapozza, C., Seppi, R., and Zischg, A. An inventory of permafrost evidence for the European Alps, Cryosphere, 5, 651–657, https://doi.org/10.5194/tc-5-651-2011, 2011.

Degenhardt, J. Development of tongue-shaped and multilobate rock glaciers in alpine environments: Interpretations from ground penetrating radar surveys, Geomorphology, 109, 94–107, https://doi.org/10.1016/j.geomorph.2009.02.020, 2009.

Delaloye, R., Reynard, E., and Wenker, L. Rock Glaciers, Entremon, Valais, Switzerland, Version 1. National Snow and Ice Data Center/World Data Center for Glaciology, Digital Media, https://nsidc.org/data/GGD290/versions/1, 1998.

DiLuzio, M., Johnson, G., Daly, C., Eischeid, J., and Arnold, J. Constructing retrospective gridded daily precipitation and temperature datasets for the conterminous United States, J. Appl. Meteorol. Clim., 47, 475–497, https://doi.org/10.1175/2007JAMC1356.1, 2008.

Duguay, M., Edmunds, A., Arenson, L., and Wainstein, P. Quantifying the significance of the hydrological contribution of a rock glacier – A review, GEOQuebec 2015: 68th Canadian Geotechnical Conference, 7th Canadian Permafrost Conference, 2015.

ESRI, ArcGIS Desktop: Release 10.4. Redlands, CA: Environmental Systems Research Institute, 2017.

Falaschi, D., Castro, M., Masiokas, M., Tadono, T., and Ahumada, A. Rock glacier inventory of the Valles Calchaquies Region (~ 25° S), Salta, Argentina, derived from ALOS data, Permafrost Periglac., 25, 69–75, https://doi.org/10.1002/ppp.1801, 2014.

Falaschi, D., Tadono, T., and Masiokas, M. Rock Glaciers in the Patagonian Andes: An inventory for the Monte San Lorenzo (Cerro Cochrane) Massif, 47° S, Geogr. Ann. A., 97(4), 769–777, https://doi.org/10.1111/geoa.12113, 2015.

Fegel, T., Baron, J., Fountain, A., Johnson, G., and Hall, E. The differing biogeochemical and microbial signatures of glaciers and rock glaciers, J. Geophys. Res.-Biogeo., 123, 919–932, https://doi.org/10.1002/2015JG003236, 2016.

Fountain, A., Glenn, B., and Basagic, H. The geography of glaciers and perennial snowfields in the American West, Arct. Antarct. Alp. Res., 49(3), 391–410, https://doi.org/10.1657/AAAR0017-003, 2017.

Francou, B., Fabre, D., Pouyaud, B., Jomelli, V., and Arnaud, Y. Symptoms of degradation in a tropical rock glacier, Bolivian Andes, Permafrost Periglac., 10, 91–100, https://doi.org/10.1002/(SICI)1099-1530(199901/03)10:13.0.CO;2-B, 1999.

Frauenfelder, H. Regional-scale modeling of the occurrence and dynamics of rock glaciers and the distribution of paleopermafrost. Ph.D. Dissertation, Geographisches Institut der Universitat Zurich, 2005.

Google Earth Pro, https://www.google.com/earth/versions/#download-pro, 2019.

Haeberli, W., Hallet, B., Arenson, L., Elconin, R., Humlum, O., Kaab, A., Kaufmann, V., Ladanyi, B., Matsuoka, N., Spingman, S., and Muhll, D. Permafrost creep and rock glacier dynamics, Permafrost Periglac., 14, 189–214, https://doi.org/10.1002/ppp.561, 2006.

Homer, C., Dewitz, J., Yang, L., Jin, S., Danielson, P., Xian, G., Coulston, J., Herold, N., Wickham, J., and Megown, K. Completion of the 2011 National Land Cover Database for the conterminous United States: Representing a decade of land cover change information, Photogramm. Eng. Rem. S., 81(5), 345–354, https://doi.org/10.14358/PERS.81.5.345, 2015.

Humlum, O. The geomorphic significance of rock glaciers: Estimates of rock glacier debris volumes and headwall recession rates in West Greenland, Geomorphology, 35, 41–67, https://doi.org/10.1016/S0169-555X(00)00022-2, 2000.

Imhof, M. Modelling and verification of the permafrost distribution in the Bernese Alps (Western Switzerland), Permafrost Periglac., 7(3), 267–280, https://doi.org/10.1002/(SICI)1099-1530(199609)7:3<267::AID-PPP221>3.0.CO;2-L, 1996.

Iribarren, P. and Bodin, X. Geomorphic consequences of two large glacier and rock glacier destabilizations in the Central Chilean Andes, EGU General Assembly 2010, June 2010, Vienna, Austria, 12:EGU2010-7162-4, 2010.

Janke, J. Colorado Front Range rock glaciers: Distribution and topographic characteristics, Arct. Antarct. Alp. Res., 39(1), 74–83, https://doi.org/10.1657/1523-0430(2007)39[74:CFRRGD]2.0.CO;2, 2007.

Janke, J. and Frauenfelder, R. The relationship between rock glaciers and contributing area parameters in the Front Range of Colorado, J. Quaternary Sci., 23(2), 153–163, https://doi.org/10.1002/jqs.1133, 2008.

Janke, J., Bellisario, A., and Ferrando, F. Classification of debris-covered glaciers and rock glaciers in the Andes of central Chile, Geomorphology, 241, 98–121, https://doi.org/10.1016/j.geomorph.2015.03.034, 2015.

Johnson, G. Active rock glacier inventory of the contiguous United States (PSUARGI). PANGAEA, https://doi.pangaea.de/10.1594/PANGAEA.918585, 2020

Jones, D., Harrison, S., and Anderson, K. Mountain glacier-to-rock glacier transition, Global Planet. Change, 181, 1–13, https://doi.org/10.1016/j.gloplacha.2019.102999, 2019a.

Jones, D., Harrison, S., Anderson, K., and Whalley, W. Rock glaciers and mountain hydrology: A review, Earth-Sci. Rev., 193, 66–90, https://doi.org/10.1016/j.earscirev.2019.04.001, 2019b.

Kaab, A. and Reichmuth, T. Advance mechanisms of rock glaciers, Permafrost Periglac., 16, 187–193, https://doi.org/10.1002/ppp.507, 2005.

Karl, T. and Koss, W. Regional and national monthly, seasonal and annual temperature weighted by area, 1895–1983. Historical Climatology Series 4–3, National Climatic Data Center, Asheville, NC, 1–38, https://repository.library.noaa.gov/view/noaa/10238, 1984.

Kellerer-Pirklbauer, A., Lieb, G., and Kleinferchner, H. A new rock glacier inventory of the eastern European Alps, Austrian J. Earth Sci., 105(2), 78–93, https://static.uni-graz.at/fileadmin/urbi-institute/Geographie/pictures/misc/kellerer-pirklbauer_at_al_2012_ajes.pdf, 2012.

Kenner, R. and Magnusson, J. Estimating the effect of different influencing factors on rock glacier development in two regions in the Swiss Alps, Permafrost Periglac., 28(1), 195–208, https://doi.org/10.1002/ppp.1910, 2017.

Knight, J., Harrison, S., and Jones, D. Rock glaciers and the geomorphological evolution of deglacierizing mountains, Geomorphology, 324, 14–24, https://doi.org/10.1016/j.geomorph.2018.09.020, 2019.

Kofler, C., Steger, S., Mair, V., Zebisch, M., Comiti, F., and Schneiderbauer, S. An inventory-driven rock glacier status model (intact vs. relict) for South Tyrol, Eastern Italian Alps, Geomorphology, 350, https://doi.org/10.1016/j.geomorph.2019.106887, 2020.

Konrad, S., Humphrey, N., Steig, E., Clark, D., Potter, N., and Pfeffer, W. Rock glacier dynamics and paleoclimatic implications, Geology, 27, 1131–1134, https://doi.org/10.1130/0091-7613(1999)027<1131:RGDAPI>2.3.CO;2, 1999.

Krainer, K. and Ribis, M. A rock glacier inventory of the Tyrolean Alps (Austria), Austrian J. Earth Sci., 105(2), 32–74, https://www.univie.ac.at/ajes/archive/volume_105_2/krainer_ribis_ajes_105_2.pdf, 2012.

Lambiel, C. and Reynard, E. Regional modeling of present, past and future distribution of discontinuous permafrost based in a rock glacier inventory in the Bagnes-Heremence area (western Swiss Alps), Norsk. Geogr. Tidsskr., 55, 219–233, https://doi.org/10.1080/00291950152746559, 2001.

Liu, L., Millar, C., Westfall, R., and Zebker, H. Surface motion of active rock glaciers in the Sierra Nevada, California, U.S.A., inventory and a case study using InSAR, Cryosphere, 7, 1109–1119, https://doi.org/10.5194/tc-7-1109-2013, 2013.

Lugon, R. and Stoffel, M. Rock-glacier dynamics and magnitude-frequency relations of debris flows in a high-elevation watershed: Ritigraben, Swiss Alps, Global Planet. Change, 73, 202–210, https://doi.org/10.1016/j.gloplacha.2010.06.004, 2010.

Magori, B., Urdea, P., and Onaca, A. Distribution and characteristics of rock glaciers in the Balkan Peninsula, Geogr. Ann. A, 102(4), 354-375, https://doi.org/10.1080/04353676.2020.1809905, 2020.

Matthews, J., Nesje, A., and Linge, H. Relict talus-foot rock glaciers at Øyberget, Upper Ottadalen, Southern Norway: Schmidt Hammer exposure ages and palaeoenvironmental implications, Permafrost Periglac., 24(4), 336–346, https://doi.org/10.1002/ppp.1794, 2013.

Millar, C. and Westfall, R. Rock glaciers and related periglacial landforms in the Sierra Nevada, CA, U.S.A.; inventory, distribution and climatic relationships, Quatern. Int., 188, 90–104, https://doi.org/10.1016/j.quaint.2007.06.004, 2008.

Millar, C. and Westfall, R. Geographic, hydrological, and climatic significance of rock glaciers in the Great Basin, U.S.A., Arct. Antarct. Alp. Res., 51(1), 232–249, https://doi.org/10.1080/15230430.2019.1618666, 2019.

Millar, C., Westfall, R. and Delany, D. Thermal and hydrologic attributes of rock glaciers and periglacial talus landforms: Sierra Nevada, California, U.S.A., Quatern. Int., 310, 169–180, https://doi.org/10.1016/j.quaint.2012.07.019, 2013a.

Millar, C., Westfall, R., Evenden, A., Holmquist, J., Schmidt-Gengenbach, J., Franklin, R., Nachlinger, J. and Delaney, D. Potential climatic refugia in semi-arid, temperate mountains: Plant and arthropod assemblages associated with rock glaciers, talus slopes, and their forefield wetlands, Sierra Nevada, California, U.S.A, Quatern. Int., 387, 106–121, https://doi.org/10.1016/j.quaint.2013.11.003, 2013b.

NAIP (National Agricultural Imagery Program) National Agriculture Imagery Program (NAIP) InformationSheet, Available online: http://www.fsa.usda.gov/Internet/FSA_File/naip_info_sheet_2013.pdf, 2012.

Navarro, F. and Magnusson, M. Position paper of the International Glaciological Society on standard practices regarding glacier inventories, International Glaciological Society, https://www.igsoc.org/news/igs_villaba2col_engesp20171220.pdf, December 21, 2017.

Nussear, K., Esque, T., Inman, R., Gass, L., Thomas, K., Wallace, C., Blainey, J., Miller, D., and Webb, R. Modeling Habitat of the Desert Tortoise (Gopherus agassizii) in the Mojave and Parts of the Sonoran Deserts of California, Nevada, Utah, and Arizona, U.S. Geological Survey Open-File Report 2009-1102, 2009.

Pauritsch, M., Birk, S., Wagner, T., Hergarten, S., and Winkler, G. Analytical approximations of discharge recessions for steeply sloping aquifers in alpine catchments, Water Resour. Res., 51(11), 8729–8740, https://doi.org/10.1002/2015WR017749, 2015.

Perucca, L. and Angillieri, M. Glaciers and rock glaciers' distribution at 28º SL, Dry Andes of Argentina, and some considerations about their hydrological significance, Environ. Earth Sci., 64(8), 2079–2089, https://doi.org/10.1007/s12665-011-1030-z, 2011.

Potter, N. Ice-cored rock glacier, Galena Creek, Northern Absaroka Mountains, Wyoming, Geol. Soc. Am. Bull., 83, 3025–3058, https://doi.org/10.1130/0016-7606(1972)83[3025:IRGGCN]2.0.CO;2, 1972.

PRISM (2017) Climate Group, Oregon State University, http://prism.oregonstate.edu, created 1 July 2015.

Rangecroft, S., Harrison, S., Anderson, K., Magrath, J., Castel, A., and Pacheco, P. A first rock glacier inventory for the Bolivian Andes, Permafrost Periglac., 25, 333–343, https://doi.org/10.1002/ppp.1816, 2014.

RGI Consortium, Randolph Glacier Inventory: A dataset of global glacier outlines: Version 6.0. Technical Report, Global Land Ice Measurements from Space, Boulder, Colorado, U.S.A.. Digital Media. https://doi.org/10.7265/N5-RGI-60, 2017.

Scotti, R., Brardinoni, F., Albereti, S., Frattini, P., and Crosta, G. A regional inventory of rock glaciers and protalus ramparts in the central Italian Alps, Geomorphology, 186, 136–149, https://doi.org/10.1016/j.geomorph.2012.12.028, 2013.

Senn, A. Large sample-size distribution of statistics used in testing for spatial correlation, Geogr. Anal., 8(2), 175–184, https://doi.org/10.1111/j.1538-4632.1976.tb01066.x, 1976.

Seppi, R., Carton, A., Zumiani, M., Dall'Amico, G., Zampedri, R., and Rigon, R. Inventory, distribution and topographic features of rock glaciers in the southern region of the Eastern Italian Alps (Trentino), Geogr. Fis. Din. Quat., 35(2), 185–197, https://doi.org/10.4461/GFDQ.2012.35.17 , 2012.

Sorg, A., Kaab, A., Roesch, A., Bigler, C., and Stoffel, M. Contrasting responses of Central Asian rock glaciers to global warming, Sci. Rep.-UK, 5, https://doi.org/10.1038/srep08228, 2015.

Stenni, B., Genoni, L., Flora, O., and Guglielmin, M. An oxygen isotope record from the Foscagno rock-glacier ice core, Upper Valtellina, Italian Central Alps, Holocene, 17(7), 1033–1039, https://doi.org/10.1177/0959683607082438, 2007.

Sulejman, R. Phytogeographic and syntaxonomic diversity of high mountain vegetation in Dinaric Alps (Western Balkan, SE Europe), J. Mt. Sci., 8, 767–786, https://doi.org/10.1007/s11629-011-2047-1, 2011.

Tiefelsdorf, M. The saddlepoint approximation of Moran's I's and Local Moran's Ii's reference distributions and their numerical evaluation, Geogr. Anal., 34(3), 187–206, https://doi.org/10.1111/j.1538-4632.2002.tb01084.x, 2002.

USGS. The National Elevation Dataset (NED), U.S. Geological Survey, Sioux Falls, South Dakota, https://pubs.usgs.gov/fs/2009/3053/pdf/fs2009_3053.pdf, 2017.

Wagner, T., Pleschberger, R., Kainz, S., Ribis, M., Kellerer-Pirklbauer, A., Krainer, K., Pilippitsch, R., and Winkler, G. The first consistent inventory of rock glaciers and their hydrological catchments of the Austrian Alps, Austrian J. Earth Sc., 113(1), 1-23, 23, https://doi.org/10.17738/ajes.2020.0001, 2020.

Figures

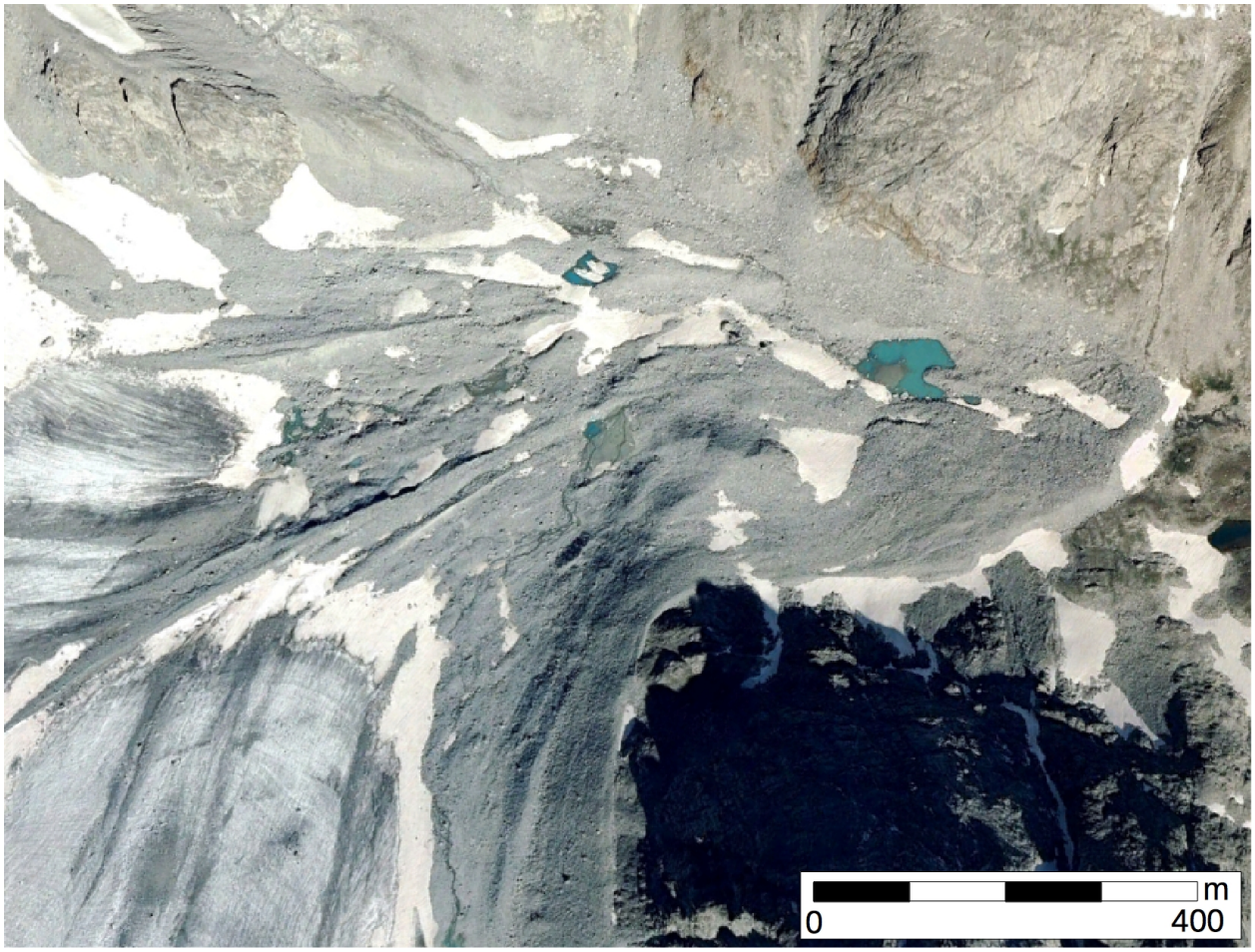

590 **Figure 1: Example of a prototypical debris-covered glacier, exhibiting expansive surfaces of exposed ice in the accumulation zone and obvious supraglacial lakes and streams on its surface. This example typifies the debris-covered glacier features we deliberately set out to exclude from this inventory. Image credit: Google Earth/Copernicus.**

595

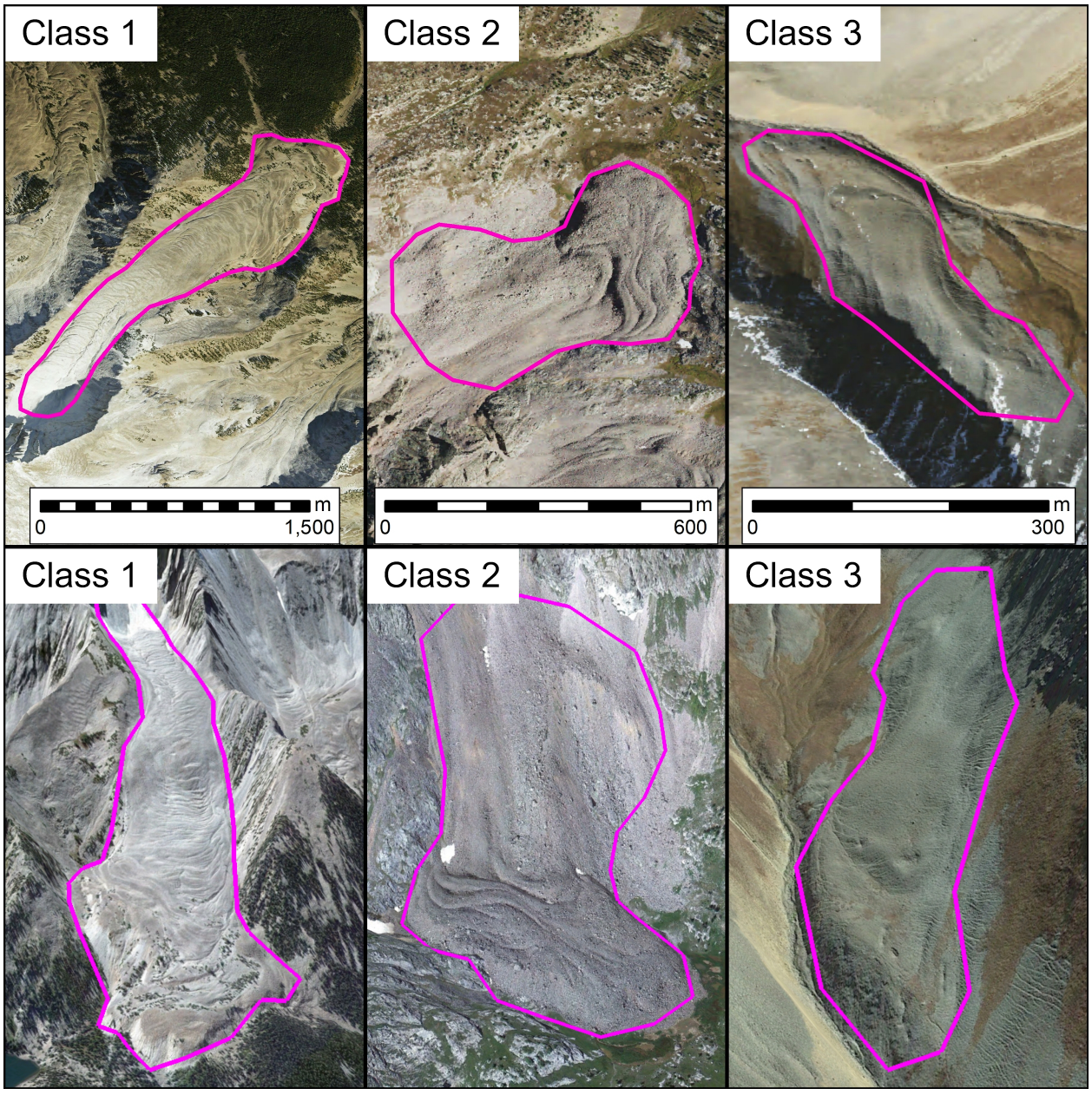

Figure 2: Examples of each of the three rock glacier classes shown in both plan view (top panels) and oblique upslope view (bottom panels). Leftmost panels show a Class 1 rock glacier (appears to be highly active, exhibits unambiguous, complex and extensive ridge and swale flow banding, and has substantially over-steepened terminal and lateral boundaries). Center panels show a Class 2 rock glacier (appears to be intermediately active, exhibits some pronounced ridge and swale flow banding, and has somewhat over-steepened terminal and lateral boundaries.). Rightmost panels show a Class 3 rock glacier (appears to be minimally active, exhibits sparse ridge and swale flow banding, and has intermittently over-steepened terminal and lateral boundaries.). Note different scale bars for each plan view panel, and that scale varies across images in oblique view panels. Image credit: Google Earth/Copernicus.

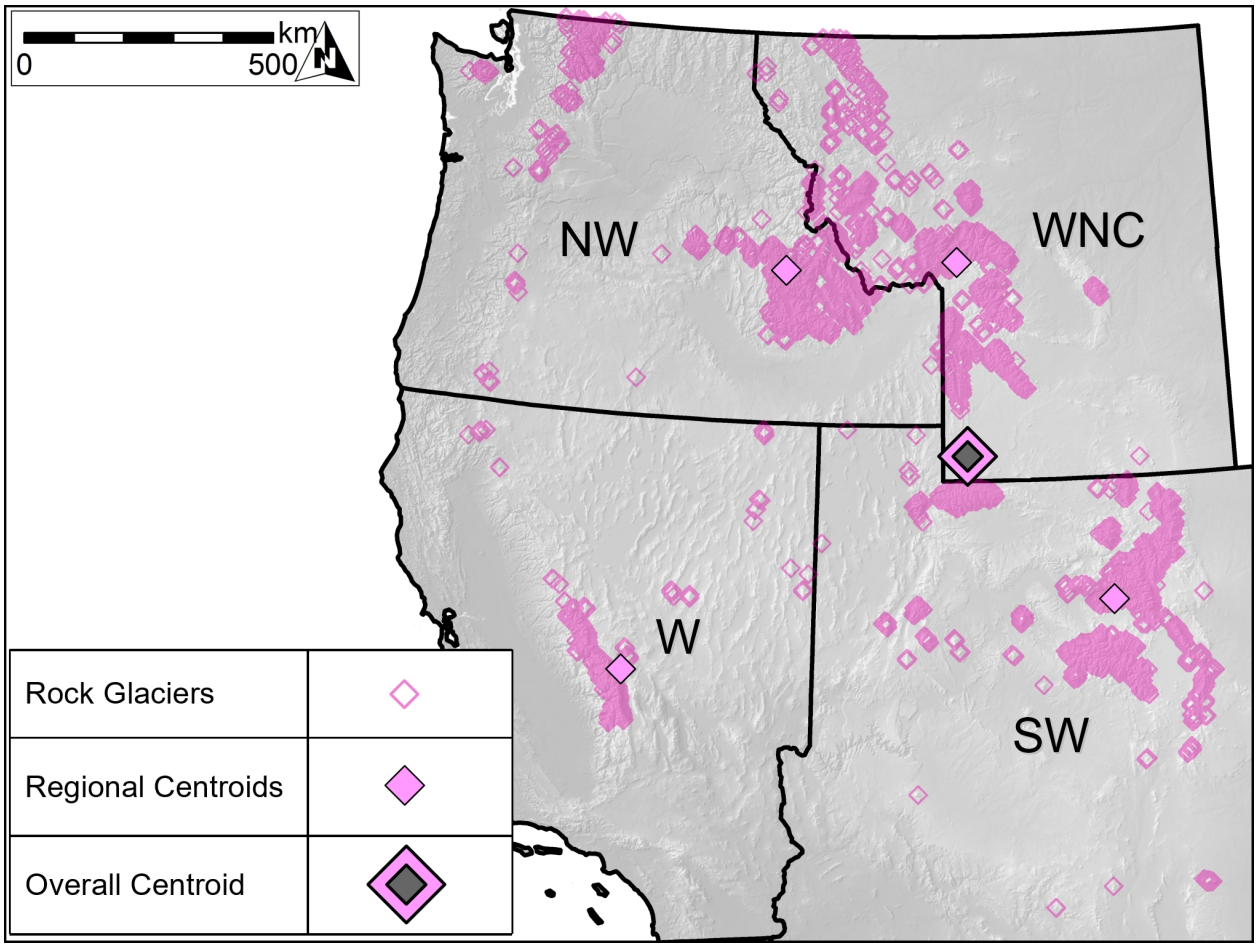

Figure 3: Locations of rock glacier inventory features (n = 10,332), as well as centroids for the entire inventory and NOAA Climate Region subsets. The largest rock glaciers, as well as highest rock glacier densities, are found in the relatively arid Southern Rocky Mountains. The Sierra Nevada of California and Uinta Mountains of Utah, climatologically similar to the Southern Rockies, also host large rock glaciers at high densities. Rock glaciers of the humid Cascade Mountains are smaller and less densely distributed, and only a few pockets of rock glaciers are found south of 35° N latitude. However, the western U.S. is generally defined by mountainous, high elevation terrain, and rock glaciers are found in all 11 western states.

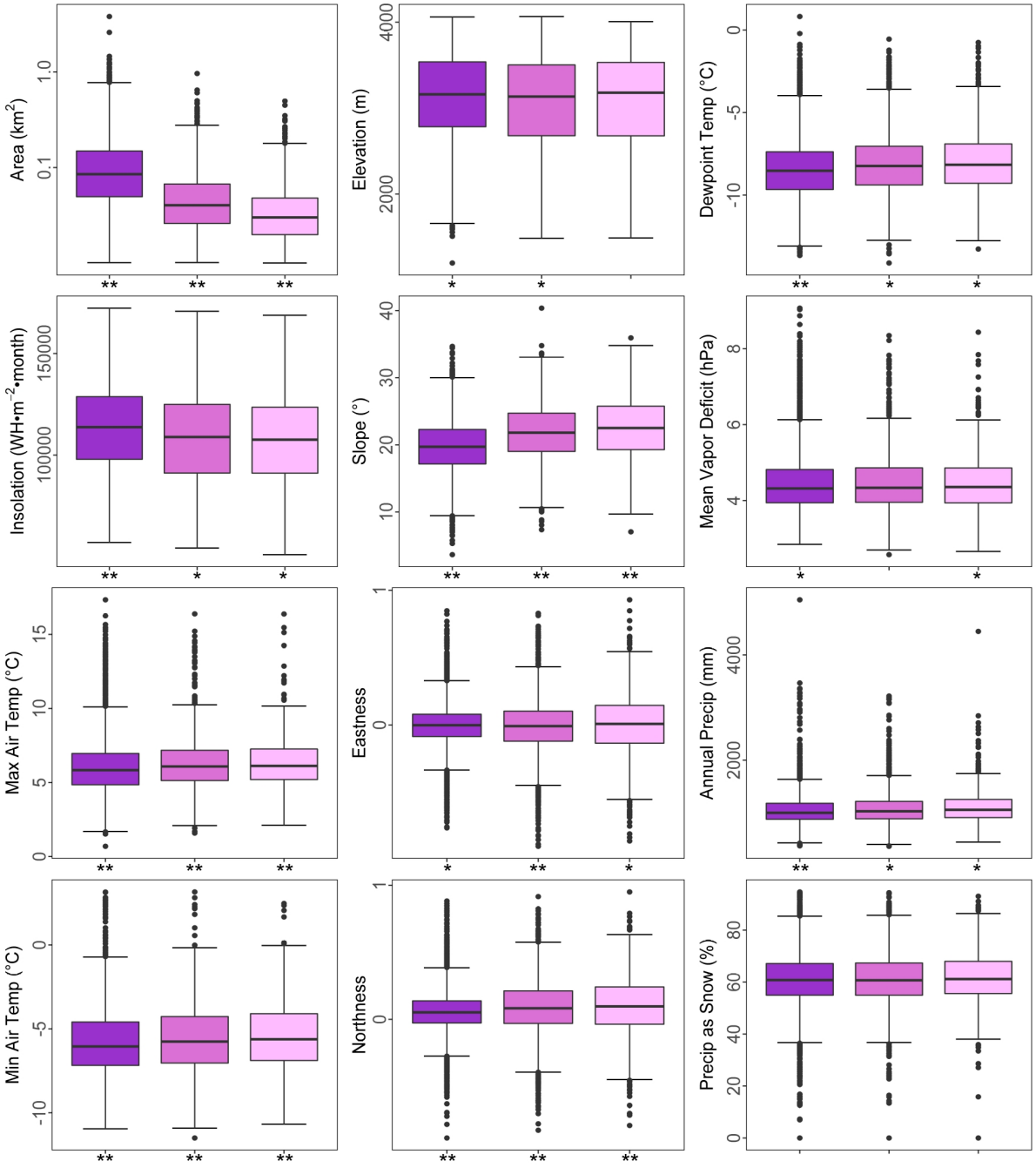

Figure 4: Geographic characteristics of Class 1 (dark purple, n = 7042), Class 2 (magenta, n = 2415) and Class 3 (light pink, n = 875) rock glaciers. Statistically significant differences (Tukey's HSD test, α = 0.05) are denoted with asterisks (different from one = *, different from both = **). Boxplot whiskers represent 1.5 times the interquartile range, outliers beyond those values are shown by solid dots.

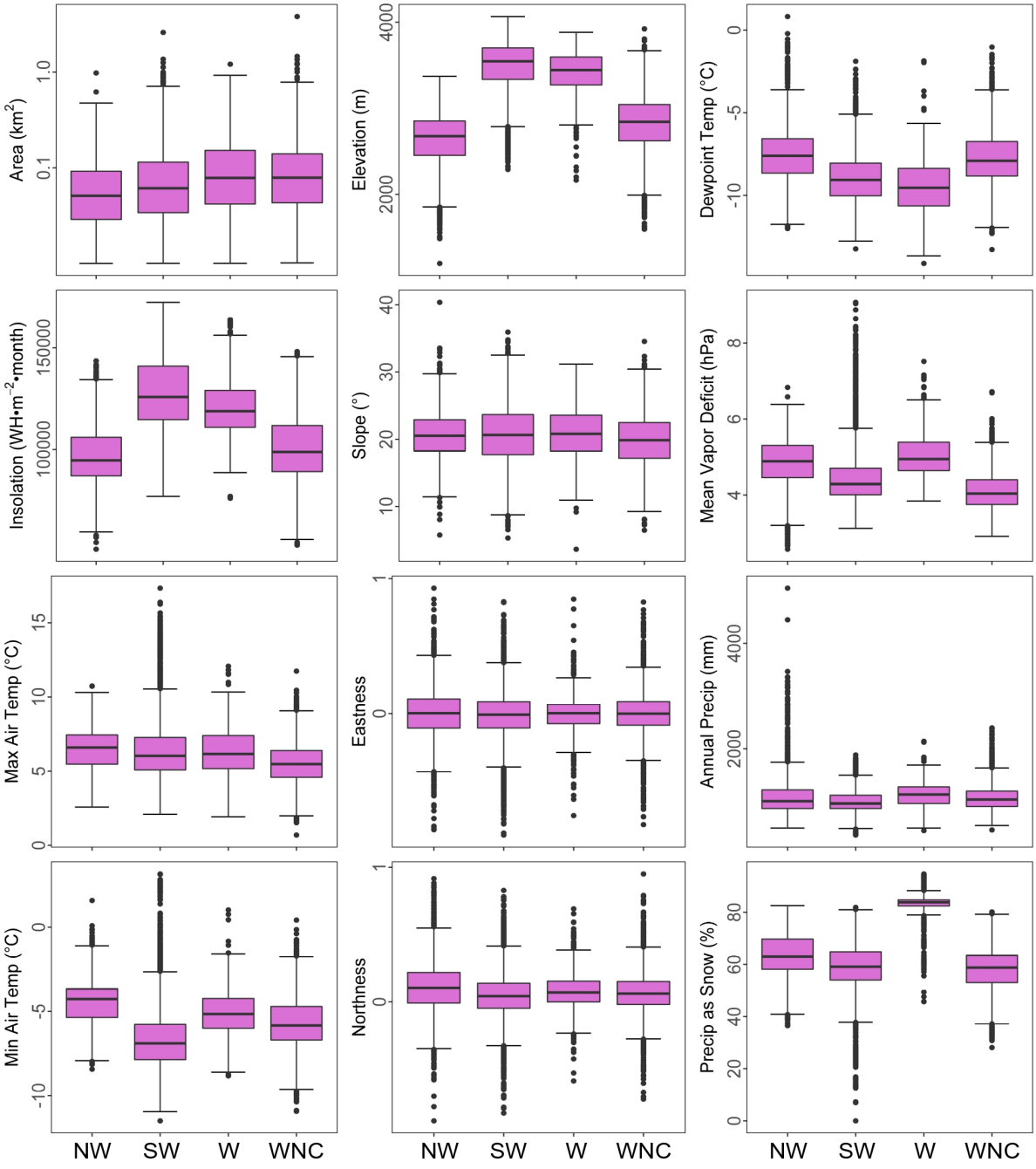

Figure 5: Geographic characteristics of rock glaciers by NOAA Climate Region. Boxplot whiskers represent 1.5 times the interquartile range, outliers beyond those values are shown by solid dots.

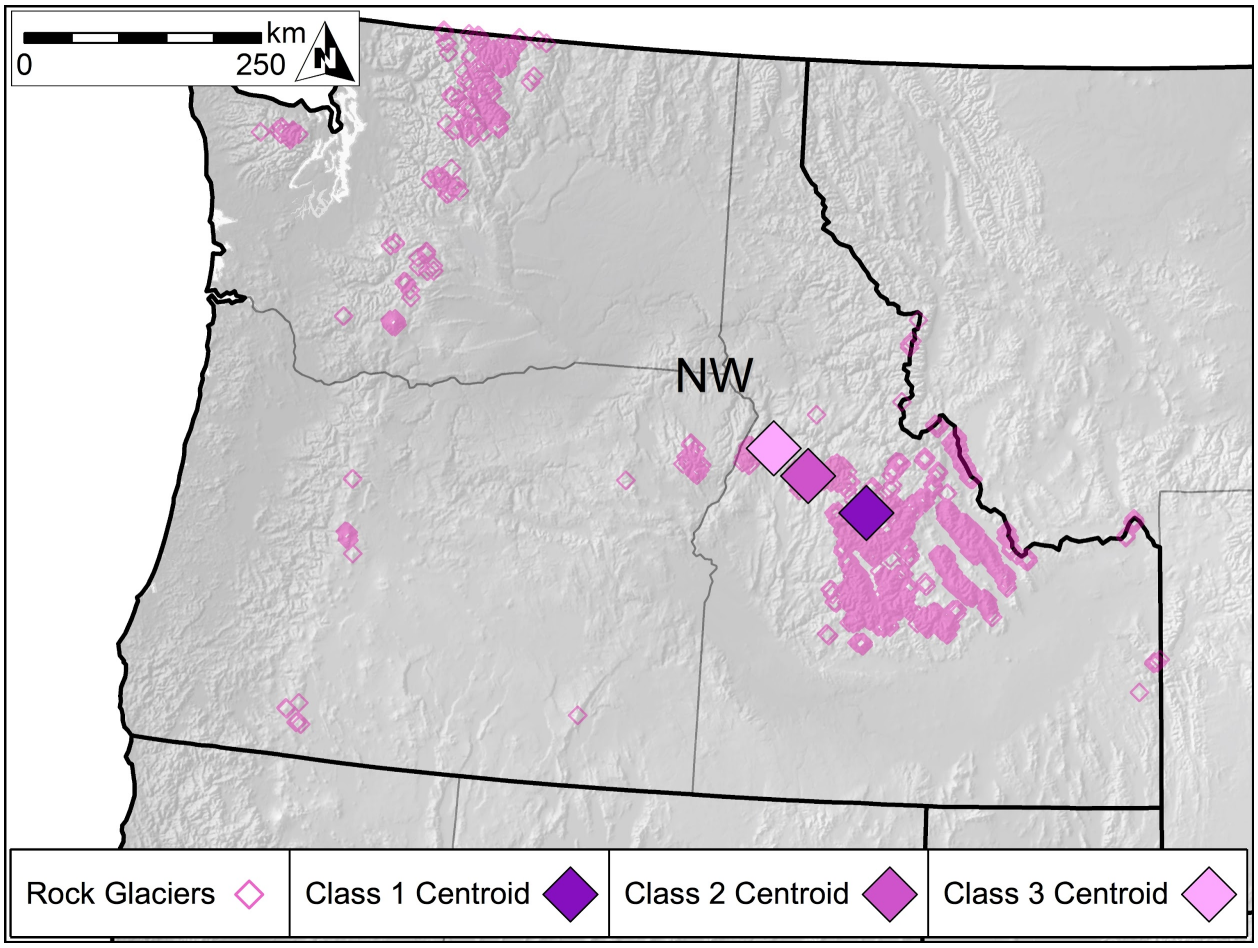

Figure 6: Locations of NW Region rock glacier inventory features (n = 1993), as well as centroids for Class 1 (n = 1293), Class 2 (n = 512) and Class 3 (n = 188) features. Rock glaciers of the NW Region are largest and most densely concentrated in the Sawtooth Mountains of Idaho.

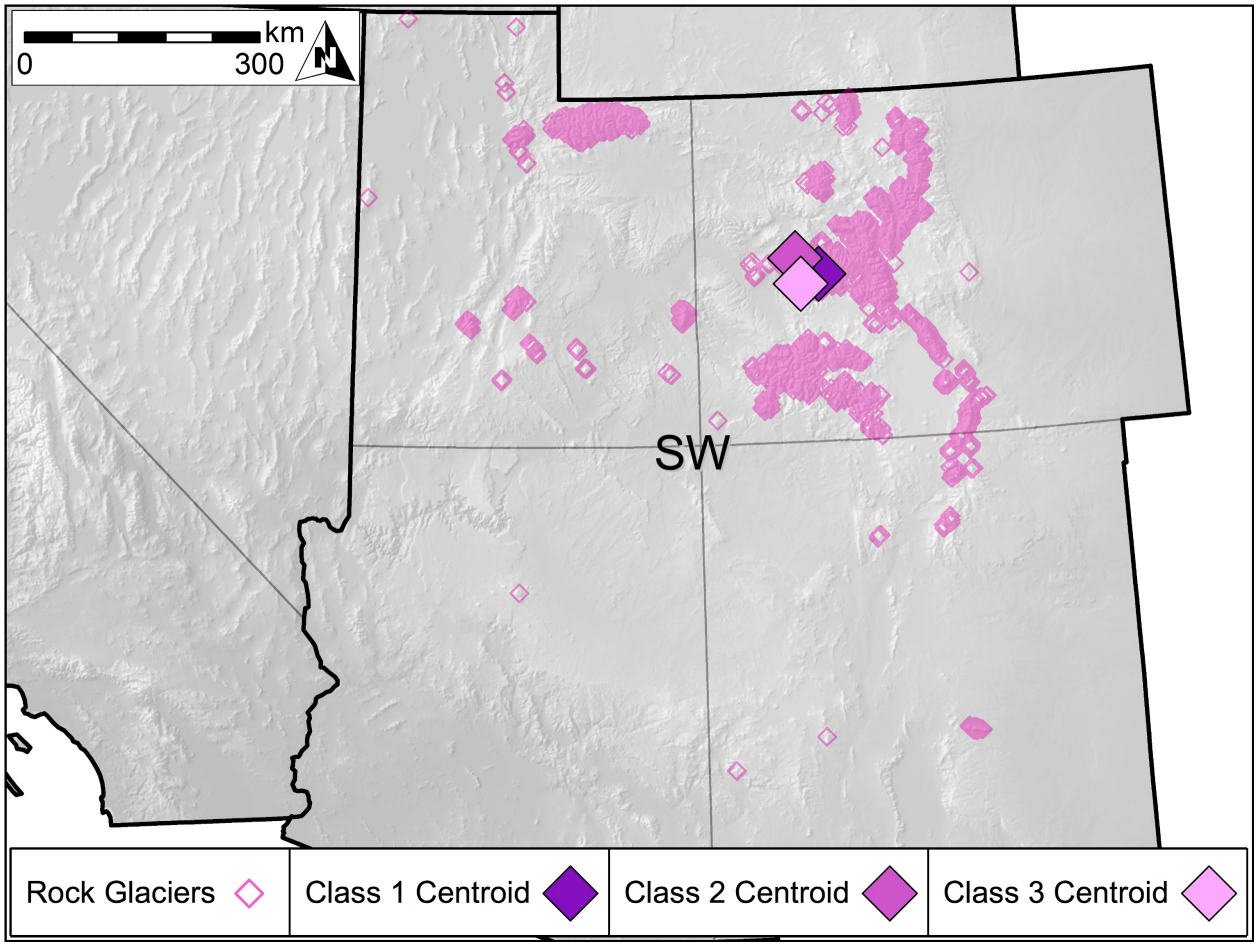

Figure 7: Locations of SW Region rock glacier inventory features (n = 4870), as well as centroids for Class 1 (n = 3291), Class 2 (n = 1133) and Class 3 (n = 446) features. Rock glaciers of the SW Region are largest and most densely concentrated in the Front Range and San Juan Mountains of Colorado and the Uinta Mountains of Utah.

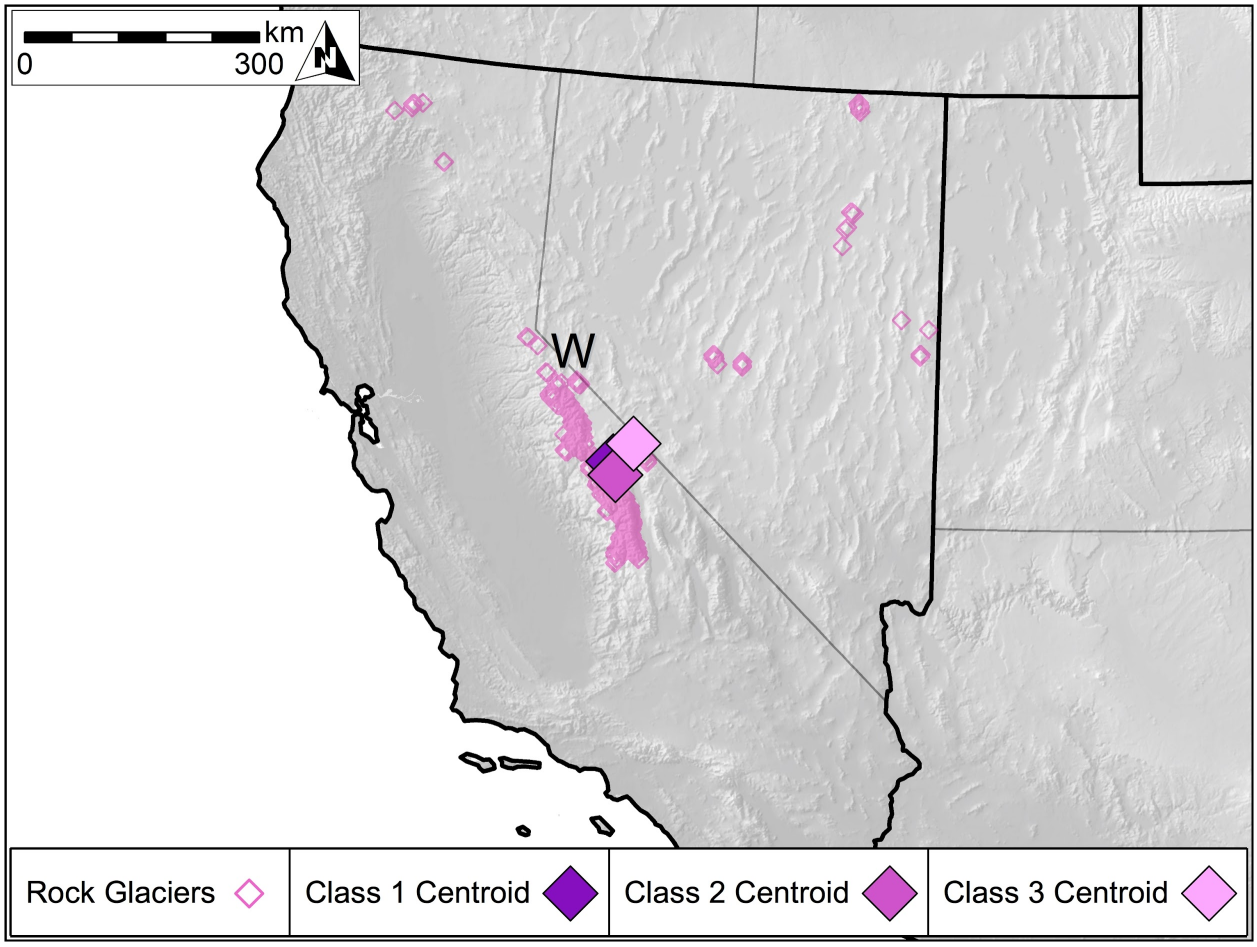

640

Figure 8: Locations of W Region rock glacier inventory features (n = 817), as well as centroids for Class 1 (n = 552), Class 2 (n = 181) and Class 3 (n = 84) features. Rock glaciers of the W Region are largest and most densely concentrated in the Sierra Nevada of California.

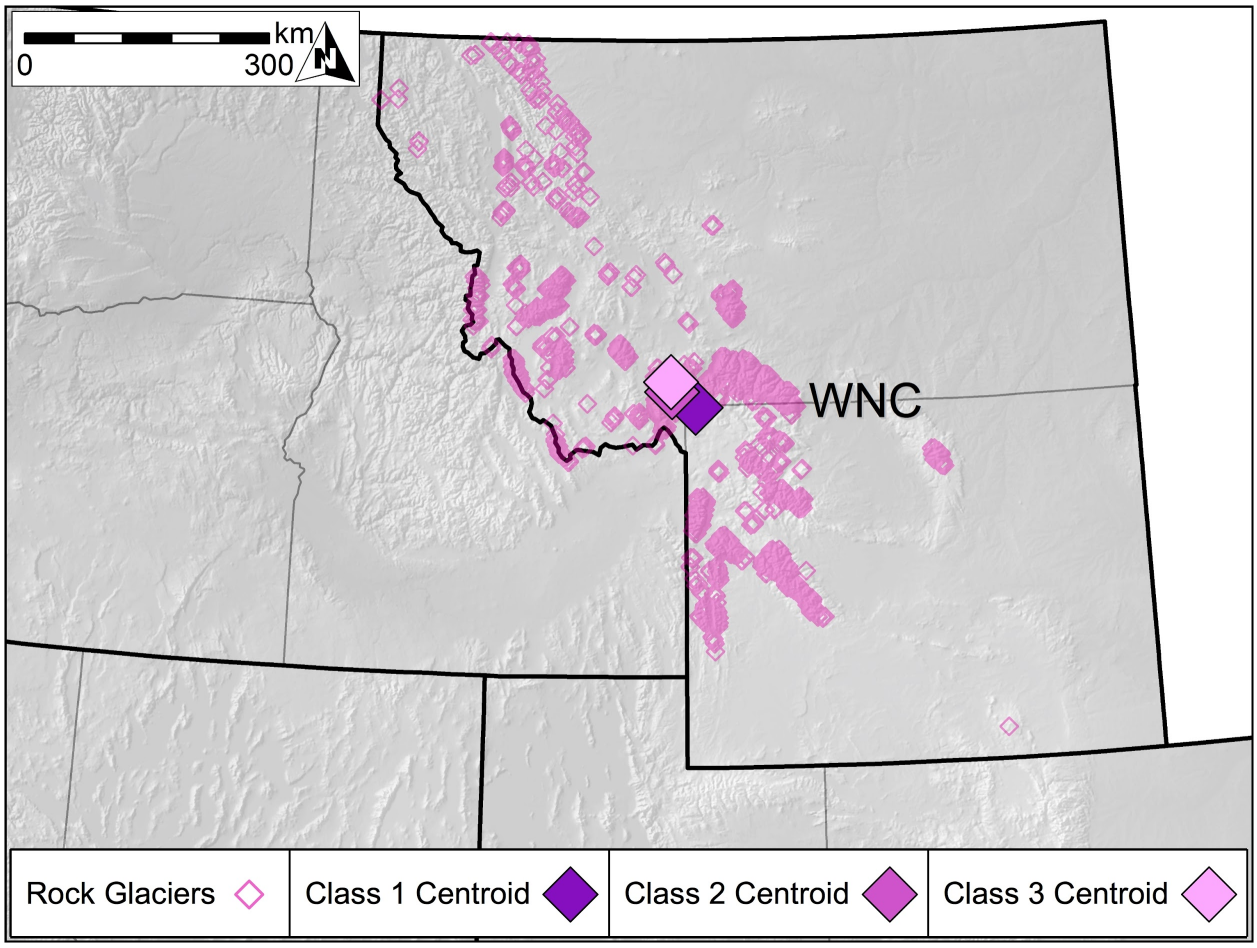

Figure 9: Locations of WNC Region rock glacier inventory features (n = 2652), as well as centroids for Class 1 (n = 1906), Class 2 (n = 589) and Class 3 (n = 157) features. Rock glaciers of the WNC Region are largest and most densely concentrated in the Beartooth Mountains of Montana and the Absaroka Range of Wyoming.

Tables

Table 1: Notable previous rock glacier inventories evaluated during comprehensive literature review. Only inventories that identified > 50 rock glaciers (i.e., at least regional scale) are included here, though sporadic smaller local inventories have been compiled.

Continent	Primary Investigator(s)	Region	Rock Glaciers Identified
Asia	Bolch and Gorbunov (2014)	Northen Tian Shan	72
Europe	Cremonese et al. (2011)	European Alps	4795
	Baroni et al. (2004)	Italian Alps	216
	Delaloye et al. (1998)	Swiss Alps	321
	Frauenfelder et al. (2005)	European Alps	84
	Imhof (1996)	Swiss Alps	80
	Keller-Pirklbauer et al. (2012)	Eastern European Alps	1647
	Kenner and Magnusson (2017)	Swiss Alps	239
	Krainer and Ribis (2012)	Austrian Alps	3145
	Lambiel and Reynard (2001)	Swiss Alps	239
	Magori et al. (2020)	Balkan Peninsula	224
	Scotti et al. (2013)	Italian Alps	1514
	Seppi et al. (2012)	Italian Alps	705
	Wagner et a. (2020)	Austrian Alps	5769
North America	Millar and Westfall (2008)	Sierra Nevada	289
	Humlum (2000)	West Greenland	400
	Janke (2007)	U.S. Rocky Mountains	220
	Janke and Frauenfelder (2008)	U.S. Rocky Mountains	180
	Liu et al. (2013)	Sierra Nevada	67
South America	Angillieri (2010)	Argentine Andes	155
	Falaschi et al. (2014)	Argentine Andes	488
	Falaschi et al. (2015)	Patagonian Andes	177

	Rangecroft et al. (2014)	Bolivian Andes	94

Table 2: Rock glacier counts by NOAA Climate Region. The SW and WNC Regions account for nearly 73% of rock glaciers identified.

NOAA Region	Class 1 (count (mean area))	Class 2 (count (mean area))	Class 3 (count (mean area))	Total Rock Glaciers (count (mean area))
NW Region	1293 (0.09 km^2)	512 (0.05 km^2)	188 (0.04 km^2)	1993 (0.07 km^2)
SW Region	3291 (0.12 km^2)	1133 (0.05 km^2)	446 (0.04 km^2)	4870 (0.09 km^2)
W Region	552 (0.16 km^2)	181 (0.06 km^2)	84 (0.05 km^2)	817 (0.12 km^2)
WNC Region	1906 (0.13 km^2)	589 (0.06 km^2)	157 (0.05 km^2)	2652 (0.11 km^2)
All Regions	7042 (0.12 km^2)	2415 (0.05 km^2)	875 (0.04 km^2)	10,332 (0.10 km^2)

Table 3: Moran's I statistics for rock glacier class. Spatial clustering is most severe in the W Region.

NOAA Region	Moran's Index	z-score	p-value	Pattern
NW Region	0.100	3.904	< 0.001	Clustered
SW Region	0.099	8.596	< 0.001	Clustered
W Region	0.176	4.179	< 0.001	Clustered
WNC Region	0.119	5.982	< 0.001	Clustered
All Regions	0.106	11.686	< 0.001	Clustered

Table 4: Moran's I statistics for rock glacier area. Spatial clustering is most severe in the W Region.

NOAA Region	Moran's Index	z-score	p-value	Pattern
NW Region	0.159	6.228	< 0.001	Clustered
SW Region	0.101	8.902	< 0.001	Clustered
W Region	0.175	4.184	< 0.001	Clustered
WNC Region	0.116	6.095	< 0.001	Clustered

All Regions	0.116	6.905	< 0.001	Clustered

Table 5: Portland State University Active Rock Glacier Inventory shapefile attribute data dictionary.

Attribute Name	Attribute Description	Attribute Units
RG_CLASS	Rock Glacier Class	Class 1, 2, or 3
AREA_KM2	Rock Glacier Area	Square Kilometers
LAT	Centroid Latitude	WGS84 Decimal Degrees
LONG	Centroid Longitude	WGS84 Decimal Degrees
STATE	Centroid U.S. State	U.S. State Abbreviation
NOAA	NOAA Climate Region	NW, SW, W, or WNC
ELEV	Elevation	Meters
SLOPE	Slope	Degrees
EAST	Aspect Eastness	Unitless
NORTH	Aspect Northness	Unitless
RAD_WIN	Average Winter (December, January, February) Solar Radiation	Watt-hours Per Square Meter
RAD_SPR	Average Spring (March, April, May) Solar Radiation	Watt-hours Per Square Meter
RAD_SUM	Average Summer (June, July, August) Solar Radiation	Watt-hours Per Square Meter
RAD_FAL	Average Fall (September, October, November) Solar Radiation	Watt-hours Per Square Meter
RAD_ANN	Average Annual Solar Radiation	Watt-hours Per Square Meter
PPT_WIN	Average Winter (December, January, February) Precipitation	Millimeters
PPT_SPR	Average Spring (March, April, May) Precipitation	Millimeters
PPT_SUM	Average Summer (June, July, August) Precipitation	Millimeters
PPT_FAL	Average Fall (September, October, November) Precipitation	Millimeters
PPT_ANN	Average Annual Precipitation	Millimeters
SNO_WIN	Average Winter (December, January, February) Snowfall	Millimeters Water Equivalent

SNO_SPR	Average Spring (March, April, May) Snowfall	Millimeters Water Equivalent
SNO_SUM	Average Summer (June, July, August) Snowfall	Millimeters Water Equivalent
SNO_FAL	Average Fall (September, October, November) Snowfall	Millimeters Water Equivalent
SNO_ANN	Average Annual Snowfall	Millimeters Water Equivalent
TDMEAN_WIN	Average Winter (December, January, February) Dewpoint Temperature	Degrees Celsius
TDMEAN_SPR	Average Spring (March, April, May) Dewpoint Temperature	Degrees Celsius
TDMEAN_SUM	Average Summer (June, July, August) Dewpoint Temperature	Degrees Celsius
TDMEAN_FAL	Average Fall (September, October, November) Dewpoint Temperature	Degrees Celsius
TDMEAN_ANN	Average Annual Dewpoint Temperature	Degrees Celsius
TMAX_WIN	Average Winter (December, January, February) Maximum Temperature	Degrees Celsius
TMAX_SPR	Average Spring (March, April, May) Maximum Temperature	Degrees Celsius
TMAX_SUM	Average Summer (June, July, August) Maximum Temperature	Degrees Celsius
TMAX_FAL	Average Fall (September, October, November) Maximum Temperature	Degrees Celsius
TMAX_ANN	Average Annual Maximum Temperature	Degrees Celsius
TMEAN_WIN	Average Winter (December, January, February) Mean Temperature	Degrees Celsius
TMEAN_SPR	Average Spring (March, April, May) Mean Temperature	Degrees Celsius
TMEAN_SUM	Average Summer (June, July, August) Mean Temperature	Degrees Celsius
TMEAN_FAL	Average Fall (September, October, November) Mean Temperature	Degrees Celsius
TMEAN_ANN	Average Annual Mean Temperature	Degrees Celsius
TMIN_WIN	Average Winter (December, January, February) Minimum Temperature	Degrees Celsius
TMIN_SPR	Average Spring (March, April, May) Minimum Temperature	Degrees Celsius
TMIN_SUM	Average Summer (June, July, August) Minimum Temperature	Degrees Celsius

TMIN_FAL	Average Fall (September, October, November) Minimum Temperature	Degrees Celsius
TMIN_ANN	Average Annual Minimum Temperature	Degrees Celsius
VPDMAX_WIN	Average Winter (December, January, February) Maximum Vapor Pressure Deficit	Hectopascals
VPDMAX_SPR	Average Spring (March, April, May) Maximum Vapor Pressure Deficit	Hectopascals
VPDMAX_SUM	Average Summer (June, July, August) Maximum Vapor Pressure Deficit	Hectopascals
VPDMAX_FAL	Average Fall (September, October, November) Maximum Vapor Pressure Deficit	Hectopascals
VPDMAX_ANN	Average Annual Maximum Vapor Pressure Deficit	Hectopascals
VPDMEAN_WI	Average Winter (December, January, February) Mean Vapor Pressure Deficit	Hectopascals
VPDMEAN_SP	Average Spring (March, April, May) Mean Vapor Pressure Deficit	Hectopascals
VPDMEAN_SU	Average Summer (June, July, August) Mean Vapor Pressure Deficit	Hectopascals
VPDMEAN_FA	Average Fall (September, October, November) Mean Vapor Pressure Deficit	Hectopascals
VPDMEAN_AN	Average Annual Mean Vapor Pressure Deficit	Hectopascals
VPDMIN_WIN	Average Winter (December, January, February) Minimum Vapor Pressure Deficit	Hectopascals
VPDMIN_SPR	Average Spring (March, April, May) Minimum Vapor Pressure Deficit	Hectopascals
VPDMIN_SUM	Average Summer (June, July, August) Minimum Vapor Pressure Deficit	Hectopascals
VPDMIN_FAL	Average Fall (September, October, November) Minimum Vapor Pressure Deficit	Hectopascals
VPDMIN_ANN	Average Annual Minimum Vapor Pressure Deficit	Hectopascals

670